BIOCHEMISTRY
including biophysical chemistry & molecular biology

Article

pubs.acs.org/biochemistry

Structural Basis for Xyloglucan Specificity and α-D-Xylp(1 → 6)-D-Glcp Recognition at the −1 Subsite within the GH5 Family

Camila Ramos dos Santos,[†,#] Rosa Lorizolla Cordeiro,[†,#] Dominic W. S. Wong,[‡] and Mário Tyago Murakami*[,†]

[†]Brazilian Biosciences National Laboratory, National Center of Research in Energy and Materials, Campinas, São Paulo 13083-970, Brazil
[‡]Western Regional Research Center, Agricultural Research Service, U.S. Department of Agriculture, Albany, California 94710, United States

Supporting Information

ABSTRACT: GH5 is one of the largest glycoside hydrolase families, comprising at least 20 distinct activities within a common structural scaffold. However, the molecular basis for the functional differentiation among GH5 members is still not fully understood, principally for xyloglucan specificity. In this work, we elucidated the crystal structures of two novel GH5 xyloglucanases (XEGs) retrieved from a rumen microflora metagenomic library, in the native state and in complex with xyloglucan-derived oligosaccharides. These results provided insights into the structural determinants that differentiate GH5 XEGs from parental cellulases and a new mode of action within the GH5 family related to structural adaptations in the −1 subsite. The oligosaccharide found in the XEG5A complex, permitted the mapping, for the first time, of the positive subsites of a GH5 XEG, revealing the importance of the pocket-like topology of the +1 subsite in conferring the ability of some GH5 enzymes to attack xyloglucan. Complementarily, the XEG5B complex covered the negative subsites, completing the subsite mapping of GH5 XEGs at high resolution. Interestingly, XEG5B is, to date, the only GH5 member able to cleave XXXG into XX and XG, and in the light of these results, we propose that a modification in the −1 subsite enables the accommodation of a xylosyl side chain at this position. The stereochemical compatibility of the −1 subsite with a xylosyl moiety was also reported for other structurally nonrelated XEGs belonging to the GH74 family, indicating it to be an essential attribute for this mode of action.

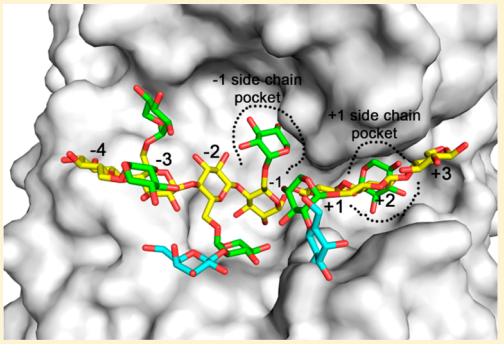

Xyloglucan is a hemicellulosic polysaccharide present in all higher plants, but predominantly in the primary cell wall of dicotyledons.[1−4] The backbone of xyloglucan consists of β-1,4-linked glucopyranosyl residues that are substituted with a regular pattern of xylosyl residues at the position 6, which may be further branched. An unambiguous nomenclature was developed to describe the structure of xyloglucan with a one-letter code given to each residue of the backbone according to its substituents[5] as follows: G, D-Glcp; X, α-D-Xylp(1 → 6)-D-Glcp; L, β-D-Galp-(1 → 2)-α-D-Xylp(1 → 6)-D-Glcp; S, α-L-Araf(1 → 2)-α-D-Xylp(1 → 6)-D-Glcp; and F, α-L-Fucp(1 → 2)-β-D-Galp-(1 → 2)-α-D-Xylp(1 → 6)-D-Glcp. The branch pattern depends on the species and tissue of origin.[6]

Xyloglucan is tightly associated with cellulose.[7] Studies have shown that xyloglucan is entrapped during the biosynthesis of cellulose microfibrils, physically connecting it to an adjacent fiber.[8] In this way, xyloglucan plays an important role in the plant cell wall morphogenesis[9] and also functions as seed storage carbohydrates.[10] Its presence in the primary cell wall of all land plants suggests that this interaction conferred an advantage in the colonization of drier habitats.[3]

Xyloglucans as well as the enzymes involved in their modification and degradation have attracted much interest not only due to their role in plant cell wall[9,11] but also by their countless biotechnological applications such as xyloglucan gels for drug delivery,[12] cellulose fiber modification,[13−15] carbohydrate-based surfactants synthesis,[16] production of oligosaccharides for cell wall analysis,[17] and most recently, conversion of plant biomass into chemical and biofuels.[18] Xyloglucan-degrading enzymes facilitate the access of cellulases and also contribute to release sugars that can be further used in fermentation.[18]

Xyloglucan-specific endo-β-1,4-glucanases (XEGs) or simply named as xyloglucanases (E.C. 3.2.1.151) are the enzymes responsible for the hydrolysis of the xyloglucan backbone. XEGs are found in the retaining families GH5, GH12, and GH16, and in the inverting families GH9, GH44, and GH74 of the Carbohydrate-Active enZYmes Database[19] (CAZy, http://www.cazy.org/ viewed on November 21, 2014). Most of the characterized XEGs act by cleaving only with an unbranched glucosyl residue (G) at the −1 subsite (based on the nomenclature for sugar-binding subsites proposed by Davies and co-workers[20]). However, some enzymes belonging to families GH74[21−24] and GH44[25] accept or prefer the xylosyl-substituted residue (X) at the −1 subsite. Two oligoxyloglucan

Received: January 5, 2015
Revised: February 23, 2015
Published: February 25, 2015

DOI: 10.1021/acs.biochem.5b00011
Biochemistry 2015, 54, 1930−1942

reducing-end-specific cellobiohydrolases (EC 3.2.1.150) from the GH74 family have also been shown to accept a xylosyl residue at the −1 subsite.[26,27] The GH5 family comprises one of the largest CAZy families with multiple activities for plant cell wall deconstruction including endo-β-1,4-glucanase (EC 3.2.1.4), licheninase (EC 3.2.1.73), cellulose β-1,4-cellobiosidase (EC 3.2.1.91), β-glucosidase (EC 3.2.1.21), endo-β-1,4-xylanase (EC 3.2.1.8), mannan endo-β-1,4-mannosidase (EC 3.2.1.78), β-mannosidase (EC 3.2.1.25), endo-β-1,6-galactanase (EC 3.2.1.164), and xyloglucan-specific endo-β-1,4-glucanase (EC 3.2.1.151). There are almost 500 members biochemically characterized and more than 50 structures available for this family (http://www.cazy.org/ viewed on November 21, 2014). However, few XEGs from the GH5 family have been functionally characterized,[21,28−31] and only two structures are known so far,[30,31] despite the biotechnological and physiological importance of these enzymes. The restricted structural information has limited our understanding of the molecular determinants for xyloglucan specificity within the GH5 family and consequently the differentiation of GH5 XEGs from homologous cellulases.[32]

Thus, in this work, we employed experimental phasing methods (SIRAS and Se-SAD) to determine the crystal structures of two novel XEGs, XEG5A, and XEG5B, retrieved from a metagenome library of bovine rumen microflora.[28,29] XEG5A is most active on tamarind xyloglucan, followed by lichenan, high degree of polymerization xyloglucan oligosaccharides (HDP-XGO), and carboxymethyl cellulose (CMC) in decreasing order, and is not active on cellulose, xylan, arabinoxylan, laminarin, or pectin.[28] XEG5B presents high specificity toward xyloglucan oligo- and polysaccharides with no detectable activity on CMC, laminarin, or lichenan.[29] XEG5A-catalyzed hydrolysis of tamarind xyloglucan produces hepta (XXXG), octa (XLXG and XXLG), and nonasaccharide (XLLG), indicating that cleavage occurred at the unbranched D-glucopyranosyl residue of the xyloglucan backbone.[28] The end products of XEG5B action on tamarind xyloglucan are smaller than heptasaccharides, and the cleavage of HDP-XGO and XXXG yields XX and XG, indicating that cleavage may occur at branched D-glucopyranosyl residues.[29] This mode of action involving the recognition of xylosyl-substituted residues at the −1 subsite is known for three GH74 members;[22,26,33] however, XEG5B is the first GH5 member with such specificity. The catalytic domains of XEG5A and XEG5B share 32% of identity, and their structures have been solved in the native state and in complex with xyloglucan-derived oligosaccharides at high resolution. The oligosaccharides bound in the negative subsites of XEG5B and in the positive subsites of XEG5A, permitted mapping of all substrate-binding subsites, for the first time, from GH5 XEGs. It revealed the structural requirements for xyloglucan specificity among GH5 members and the structural basis for XXXG cleavage into XX and XG by XEG5B, which involves a modification in the −1 subsite enabling the accommodation of a xylosyl side chain at this position.

MATERIALS AND METHODS

Molecular Cloning and Production of the XEG5B Catalytic Domain. The nucleotide sequence encoding the XEG5B catalytic domain ($XEG5B_{CD}$) was amplified from the pET32-XEG5B plasmid[29] (GenBank ID: ADB44000.1) using the following oligonucleotides: forward, 5′-CCCGGGGGC-CATGGCTACCAAGGATGCCCAGGCTATTG-3′, and reverse, 5′-CTCGAGGAAAGGCCACTTGCCAGCTG-3′ and the PlatinumTaq DNA polymerase (Invitrogen, Carlsbad, CA). The PCR product was cloned into the pGEM-T Easy cloning vector (Promega, Madison, WI), sequenced, and further subcloned into the bacterial expression vector pET28a (EMD Biosciences, San Diego, CA) using the *NcoI* and *XhoI* restriction sites. *Escherichia coli* BL21(DE3) cells (New England BioLabs, Woburn, MA), transformed with the pET28a-XEG5B plasmid, were grown in 1 L of LB medium (10 g/L tryptone, 10 g/L sodium chloride and 5 g/L yeast extract), supplemented with 50 μg/mL kanamycin at 37 °C and 200 rpm. When the culture reached an $OD_{600\ nm}$ of 0.6, the expression was induced with 0.1 mM IPTG for 4 h at 30 °C and 200 rpm.

Overexpression of Native and Se-Met XEG5A. *E. coli* BL21(DE3) cells, harboring the pET32b-XEG5A[28] plasmid (GenBank ID: ACZ54907.1), were grown in 1 L of LB medium, supplemented with 100 μg/mL ampicillin at 37 °C and 200 rpm. When the culture reached an OD_{600nm} of 0.6, the expression was induced with 0.1 mM IPTG for 4 h at 30 °C and 200 rpm. The Se-Met protein was produced according to the method described by Doublié,[34−36] in which a nonauxotrophic strain is used by inhibiting methionine biosynthesis. In this protocol, *E. coli* BL21(DE3) cells harboring the pET32b-XEG5A[28] plasmid were grown in M9 minimal medium (68 g/L sodium phosphate dibasic, 30 g/L potassium phosphate monobasic, 5 g/L sodium chloride, 2 mM magnesium sulfate, 37 mM ammonium chloride, 0.2 mM calcium chloride, and 0.05 mM ferric chloride), supplemented with 1% (w/v) glucose, 1% (w/v) thiamin, and 100 μg/mL ampicillin, at 37 °C and 200 rpm. When the culture reached an OD_{600nm} of 0.6, it was supplemented with a sterile mixture of amino acids (lysine, phenylalanine, and threonine at 1 mg/mL, isoleucine, leucine, and valine at 0.5 mg/mL, and selenomethionine at 0.6 mg/mL), and the expression was induced with 0.1 mM IPTG for 4 h at 30 °C and 200 rpm. Amino acids were purchased from Sigma-Aldrich (St. Louis, MO).

Protein Purification. Cells were harvested by centrifugation at 6000*g* for 30 min (4 °C) and further resuspended in 20 mL of buffer A (20 mM Na_2HPO_4 and 0.5 M NaCl, pH 7.5) supplemented with protease inhibitors (1 mM PMSF and 5 mM benzamidine). Cell lysis was performed by chemical (2 μg/mL lysozyme, 15 min, on ice) and physical (sonication, 10 pulses of 30% amplitude for 15 s, on ice, Sonic Sonifier, tip 360-0420) treatments. The cell extract was clarified by centrifugation (20000*g*, 30 min, 4 °C) and applied onto 5 mL Hi-Trap chelating column (GE Healthcare Biosciences, Pittsburgh, PA) equilibrated with buffer A using an ÄKTA system (GE Healthcare Biosciences, Pittsburgh, PA). After extensive washing with buffer A, bound proteins were eluted with a nonlinear gradient of buffer B (20 mM Na_2HPO_4, 0.5 M NaCl and 0.5 M imidazole, pH 7.5). XEG5A (native and Se-Met derivative) eluted as a single peak with two distinct populations according to SDS-PAGE analysis. These samples correspond to the full-length XEG5A in fusion with thioredoxin (TRX) and His-tag (named as TRX-XEG5A), and to the His-tagged catalytic domain ($XEG5A_{CD}$), indicating endogenous proteolytic cleavage. $XEG5B_{CD}$ eluted as a single peak with the expected molecular weight for the catalytic domain with His-tag. Fractions of each peak were pooled and concentrated to 1 mL using Amicon Ultra centrifugal units (EMD Biosciences, San Diego, CA). The concentrated samples were further purified on a Superdex 75 16/60 column (GE Healthcare Biosciences, Pittsburgh, PA), equilibrated with phosphate buffer (20 mM Na_2HPO_4 and 0.15 M NaCl, pH 7.5), at a flow

DOI: 10.1021/acs.biochem.5b00011
Biochemistry 2015, 54, 1930−1942

rate of 0.5 mL/min. TRX-XEG5A and $XEG5A_{CD}$ were successfully separated by size-exclusion chromatography and showed high purity and homogeneity according to SDS-PAGE and dynamic light scattering analyses, respectively. Fractions of each peak containing pure and homogeneous protein were pooled, dialyzed against 20 mM HEPES buffer (pH 7.5), and concentrated by ultrafiltration to 15 mg/mL (Se-Met TRX-XEG5A), 12 mg/mL (Se-Met $XEG5A_{CD}$), and 18 mg/mL ($XEG5B_{CD}$). Protein concentration was estimated by A_{280nm} using the respective extinction coefficients of each construct: 99810, 84340, and 83310 M^{-1} cm^{-1} for TRX- XEG5A, $XEG5A_{CD}$, and $XEG5B_{CD}$, respectively.

Site-Directed Mutagenesis. The single (D405A) and the triple (Y323A/D405A/F407A) mutants of XEG5A were constructed using the QuikChange multi site-directed mutagenesis kit (Agilent Technologies, Santa Clara, CA). Primers were designed using the QuikChange Primer Design program. The mutations were confirmed by DNA sequencing. BL21(DE3)-plyE cells harboring the mutant plasmids were cultured in selective LB medium at 30 °C overnight, followed by 37 °C for 5.5 h. Protein expression was carried out by the addition of 1 mM IPTG and cultured further at 18 °C for 16 h. The harvested cell pellet (~1.5 g) was treated with a mixture of Cellulytic B (15 mL/g cell), lysozyme (0.2 mg/mL), benzonase (50 U/mL), and protease inhibitor cocktail (Roche Molecular Biochemicals, Indianapolis, IN). The extracted protein was purified using a Ni-Sepharose column (20 mM Na_2HPO_4, 0.5 M NaCl, 10−300 mM imidazole gradient). Activity assays were performed with AZCL xyloglucan as the substrate (Megazyme, Wicklow, Ireland). Active fractions were combined and further purified using a Q-Sepharose FF column (GE Healthcare Biosciences, Pittsburgh, PA) and a NaCl gradient (up to 0.25 M) in 20 mM Bis-Tris buffer, pH 6.2. Active fractions were pooled, concentrated, and buffer-exchanged into the initial buffer with added 10% (v/v) glycerol. The purified mutant enzymes appeared as single bands on SDS-PAGE.

Thin-Layer Chromatography. Enzymatic reactions of the wild-type and mutant enzymes were measured by monitoring the formation of small oligomeric products using thin-layer chromatography. The reaction mixture consisted of 5 μg of enzyme and substrate (0.5% (w/v) heptasaccharide XXXG (Megazyme, Wicklow, Ireland), 0.5% (w/v) HDP-XGO (Megazyme, Wicklow, Ireland) or 1% (w/v) tamarind xyloglucan (Megazyme, Wicklow, Ireland)) in 50 μL of phosphate buffer (50 mM K_2HPO_4, pH 7.0), incubated at 37 °C for 1 h. The reaction mixture was applied onto a HPTLC silica gel plate, developed with a mobile phase of 1-PrOH/CH_3CN/HOAc (7:1:2), and visualized by spraying with 10% (v/v) H_2SO_4 and 1 mg/mL orcinol in methanol.

Crystallization. Crystallization trials were performed by the sitting-drop vapor-diffusion method using a Cartesian Dispensing System (HoneyBee 963, Digilab, Marlborough, MA). The drops consisting of a mixture of 0.5 μL of protein solution and an equal volume of reservoir solution were equilibrated against 80 μL of mother liquor at 18 °C. Small single crystals of Se-Met $XEG5A_{CD}$ were obtained in 25% (w/v) PEG3350, 20% (v/v) PEG400, 0.1 M $MgCl_2$ and 0.1 M Tris-HCl, pH 8.5. Large crystals (600 × 150 × 150 μm^3) were grown after reduction of PEG3350 concentration to 12% (w/v) in hanging drops prepared with 1 μL of protein solution and 1 μL of reservoir solution. In some cases, the Tris-HCl buffer of the mother liquor was replaced by PCB, which is a buffer produced by mixing sodium propionate ($C_3H_5NaO_2$), sodium cacodylate ($C_2H_7AsO_2$), and BIS-TRIS propane ($C_{11}H_{26}N_2O_6$) in a molar ratio of 2:1:2, respectively. $XEG5B_{CD}$ crystallized in several conditions, and clusters of 3D crystals were observed in the condition 2 M ammonium sulfate ($(NH_4)_2SO_4$) and 0.1 M trisodium citrate ($Na_3C_6H_5O_7$), pH 5.5. The addition of 5% (v/v) glycerol in the condition and changing the temperature to 4 °C resolved the cluster formation. However, large single crystals (500 × 300 × 150 μm^3) were only attained when the drop volume was increased to 2 μL in hanging-drop format.

Data Collection and Processing. Se-Met $XEG5A_{CD}$ crystal was directly flash cooled in an 100 K nitrogen gas stream. The Blu-Ice program[37] was used to scan the X-ray energy against the fluorescence emitted by the sample and the AUTOCHOOCH program[38] automatically calculated the anomalous scattering factors from the fluorescence data. X-ray diffraction data were collected at the energy of 12 663 eV, corresponding to the maximum of f'' (peak). $XEG5A_{CD}$ in complex with xyloglucan-derived oligosaccharides and Tris was obtained by soaking crystals for 7 h with 10 mM of a mixture of hepta- (XXXG), octa- (XLXG/XXLG), and nona-saccharides (XLLG) (Megazyme, Wicklow, Ireland). The glucose complex was attained by soaking crystals with 10 mM glucose (Sigma-Aldrich, St. Louis, MO) for 18 h. $XEG5A_{CD}$ crystals, grown in PCB buffer instead of Tris, were incubated with the same mixture of xyloglucan-derived oligosaccharides, glucose, and cellotriose (Megazyme, Wicklow, Ireland) (10 mM each) for 1 h. Native $XEG5B_{CD}$ crystals were cryoprotected by soaking in the mother liquor supplemented with 20% (v/v) glycerol for 10 s before flash cooling. $XEG5B_{CD}$ crystals were derivatized by the quick cryosoaking method.[39] They were soaked in the mother liquor solution containing 0.5 M sodium iodide (NaI) and 20% (v/v) glycerol for 20 s. $XEG5B_{CD}$ in complex with XXLG was obtained by soaking crystals with 10 mM xyloglucan-derived oligosaccharides for 18 h. All data sets were collected on the W01B-MX2 beamline at the Brazilian Synchrotron Light Laboratory (LNLS, Campinas, Brazil)[40] and processed and merged with XDS[41] using the $CC_{1/2}$ criterion (>0.5) for high-resolution cutoff.[42]

Structure Solution and Refinement. The native structure of $XEG5A_{CD}$ was solved by the single anomalous dispersion (SAD) method using the diffraction data from the Se-Met crystal. The programs SHELXD and SHELXE[43] were used for heavy atom location and phase calculation, respectively. The model was initially built with the AutoBuild wizard[44] from the PHENIX package. The structure of $XEG5A_{CD}$ in complex with ligands was solved by molecular replacement method with the program MolRep[45] using the refined native structure of $XEG5A_{CD}$ as template. The native structure of $XEG5B_{CD}$ was elucidated by the single isomorphous replacement with anomalous scattering (SIRAS) method using the same programs and routines applied to $XEG5A_{CD}$ phasing. All structures were refined with the program REFMAC5[46] and manually inspected using the program COOT.[47] The refined structures were evaluated using the program MolProbity.[48] Data collection, processing, and refinement statistics are summarized in Table 1.

RESULTS AND DISCUSSION

XEG5A Has Higher Structural Similarity to Cellulases than to GH5 Xyloglucanases. $XEG5A_{CD}$ structure could not be solved by molecular replacement methods, even if combined with structure modeling and crystallographic model-building techniques.[49] Crystal derivatization according to the quick

DOI: 10.1021/acs.biochem.5b00011
Biochemistry 2015, 54, 1930−1942

Table 1. Data Collection and Refinement Statistics of $XEG5A_{CD}$ and $XEG5B_{CD}$ Structures

	XEG5A (native)	XEG5A (glucose)	XEG5A (glucose and Tris)	XEG5A (XGG)	XEG5A (XLG and Tris)	XEG5A (cellotriose)	XEG5B (iodine derivative)	XEG5B (native)	XEG5B (XXLG/XXG)
Data collection									
wavelength (Å)	0.932	1.459	1.459	1.459	1.459	1.459	1.458	0.954	0.954
space group	$P3_1$	$P3_1$	$P3_1$	$P3_1$	$P3_1$	$P3_1$	$P6_1$	$P6_1$	$P6_1$
cell dimensions									
a, *b*, *c* (Å)	97.24, 97.24, 95.68	97.60, 97.60, 96.24	96.95, 96.95, 95.78	96.50, 96.50, 95.86	97.66, 97.66, 95.98	96.70, 96.70, 95.72	121.15, 121.15, 59.10	120.95, 120.95, 59.03	120.63, 120.63, 59.00
α, β, γ (deg)	90.00, 90.00, 120.00	90.00, 90.00, 120.00	90.00, 90.00, 120.00	90.00, 90.00, 120.00	90.00, 90.00, 120.00	90.00, 90.00, 120.00	90.00, 90.00, 120.00	90.00, 90.00, 120.00	90.00, 90.00, 120.00
resolution (Å)	50.00−1.79 (1.89−1.79)[a]	50.00−1.92 (2.03−1.92)	50.00−2.64 (2.80−2.64)	50.00−2.15 (2.28−2.15)	50.00−1.58 (1.67−1.58)	50.00−2.40 (2.55−2.40)	50.00−2.00 (2.03−2.00)	50.00−1.72 (1.82−1.72)	50.00−1.15 (1.22−1.15)
R_{meas}	0.114 (1.678)	0.160 (1.816)	0.141 (1.462)	0.223 (1.350)	0.133 (1.742)	0.211 (1.425)	0.139 (0.202)	0.046 (0.172)	0.056 (0.294)
$I/\sigma I$	11.95 (1.16)	12.81 (1.43)	16.01 (1.64)	7.72 (1.42)	10.43 (1.35)	10.01 (1.57)	9.23 (8.77)	45.99 (14.40)	26.38 (6.86)
CC1/2	0.99 (0.52)	0.99 (0.55)	0.99 (0.65)	0.99 (0.51)	0.99 (0.59)	0.99 (0.62)		0.99 (0.99)	0.99 (0.96)
completeness (%)	99.3 (96.3)	96.0 (83.4)	96.7 (81.5)	97.6 (96.1)	99.3 (97.6)	97.9 (96.4)	98.3 (96.5)	96.9 (83.9)	95.7 (85.9)
redundancy	5.5 (5.2)	10.7 (8.8)	10.8 (8.6)	5.4 (5.3)	10.4 (9.5)	5.5 (5.5)	6.9 (6.7)	10.6 (8.7)	8.3 (6.7)
heavy atom sites	10						21		
FOM[b]	0.757						0.727		
Refinement									
resolution (Å)	31.61−1.79	48.85−1.92	48.52−2.64	43.14−2.15	43.56−1.58	43.20−2.40		42.28−1.72	39.49−1.15
no. reflections	50382	71581	27243	50382	132766	36412		49509	157480
R_{work}/R_{free}	0.178/0.202	0.179/0.216	0.214/0.236	0.188/0.233	0.125/0.162	0.221/0.256		0.105/0.149	0.103/0.122
No. atoms									
protein	5388	5385	5380	5380	5407	5380		3012	3044
ligand/ion	16/2	24/2	24/16/2	86/2	106/16/2	68/2		18/20	85/52/12/15
water	467	418	63	285	601	93		493	678
protein residues	678 (2 chains)	678 (2 chains)	678 (2 chains)	678 (2 chains)	679 (2 chains)	678 (2 chains)		386 (1 chain)	386 (1 chain)
ligand/ion	Tris/Mg^{2+}	glucose/Mg^{2+}	glucose/Tris/Mg^{2+}	XGG/Mg^{2+}	XLG/Tris/Mg^{2+}	cellotriose/Mg^{2+}		glycerol/sulfate	XXLG/XXG/ glycerol/sulfate
B-factors (Å^2)									
average	28.0	29.0	64.0	31.0	25.0	40.0		12.0	11.0
protein	27.9	29.5	64.6	30.7	24.0	40.2		10.1	7.9
ligand/ion	38.7/33.6	53.5/40.5	95.6/83.8/72.7	58.6/41.1	43.3/27.9/28.8	65.0/50.9		28.4/23.8	14.3/23.9/24.1/12.5
water	34.3	33.8	57.1	31.1	35.5	35.1		23.1	26.5
r.m.s. deviations									
bond lengths (Å)	0.007	0.019	0.004	0.017	0.020	0.005		0.020	0.025
bond angles (deg)	0.975	1.794	0.877	1.776	2.129	0.928		1.849	2.192
Ramachandran									
favored (%)	96	96	95	95	96	95		96	97
outliers (%)	0	0	0	0	0	0		0	0
PDB code	4W84	4W85	4W86	4W87	4W88	4W89		4W8A	4W8B

[a]Values in parentheses are for highest-resolution shell. [b]Mean figure of merit after density modification with program SHELXE.

DOI: 10.1021/acs.biochem.5b00011
Biochemistry 2015, 54, 1930−1942

cryosoaking method[39] with iodide and cesium ions was unsuccessful due to crystal dissolution in the presence of such salts. Then, its three-dimensional structure was only determined by the SAD method with Se-Met crystals. Two protein chains were found in the asymmetric unit, forming an interface stabilized by magnesium ions (Figure S1A, Supporting Information). These ions make several water-mediated contacts with both protomers, exhibiting an octahedral coordination cage (Figure S1B), which probably contributed to a well-ordered and stable periodic crystalline arrangement. However, this interface is likely a crystallization artifact since size-exclusion chromatography and dynamic light scattering indicated that $XEG5A_{CD}$ is a monomer in solution (results not shown).

$XEG5A_{CD}$ structure comprises the classical $(\beta/\alpha)_8$-barrel (Figure 1A) and as expected for proteins with this fold, the substrate binding region is located at the carboxy-terminal ends of the β-strands, being formed by the loops that connect β and α elements of the barrel (Figure 1A). The eight invariant residues of GH5 enzymes,[50,51] which are Arg150, His194, Asn239, Glu240, His314, Tyr316, Glu362, and Trp395 (XEG5A sequence numbering), are also conserved in XEG5A (Figures 1A and S2). In this context, by analogy with other GH5 enzymes, the catalytic residues are Glu240 (acid/base) and Glu362 (nucleophile).

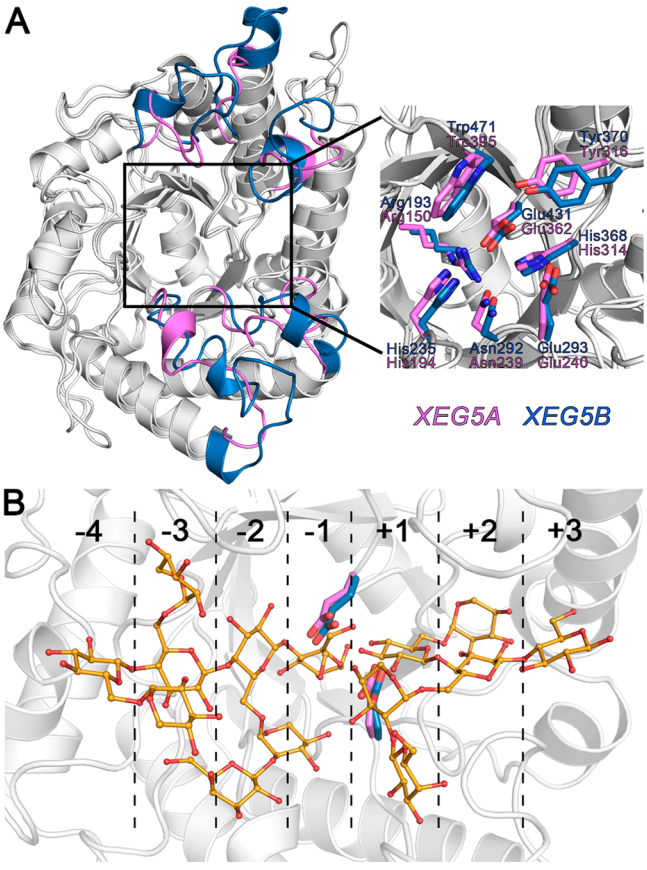

Figure 1. Overall structures of $XEG5A_{CD}$ and $XEG5B_{CD}$. (A) Their structures were superposed and the main differences in the catalytic interface are colored in pink (XEG5A) and blue (XEG5B) (left). The eight fully conserved residues in the GH5 family are shown (right) in the same color pattern. (B) The ligands in the negative subsites of XEG5B and in the positive subsites of XEG5A are shown to delineate the subsites from −4 to +3. Catalytic residues of XEG5A and XEG5B are also depicted. The structures are in similar orientations in panels A and B.

According to the classification proposed by Henrissat and co-workers,[52] XEG5A belongs to the subfamily 4, which is the only subfamily enclosing XEGs. However, within this subfamily, XEG5A showed higher similarity to cellulases than to XEGs. Among the structurally characterized GH5_4 members, the most similar enzymes are the endoglucanase from *Piromyces rhizinflata* (PrEglA;[53] PDB ID: 3AYR; r.m.s.d. 1.3 Å, 335 Cα atoms, 39% ident.) and the multifunctional cellulase, xylanase and mannanase from *Clostridium thermocellum* (CtMult, PDB ID: 4IM4; r.m.s.d. 1.3 Å, 328 Cα atoms, 41% ident.). The two XEGs from *Paenibacillus pabuli* (PpXG5,[30] PDB ID: 2JEQ) and *Bacteroides ovatus* (BoGH5A,[31] PDB ID: 3ZMR), share 34 and 30% of identity with XEG5A, respectively, and they resulted in an r.m.s.d. of 2.0 Å when superposed to $XEG5A_{CD}$. The fact that XEG5A is more similar to cellulases than to homologous XEGs indicates that xyloglucan specificity within the GH5 family is closely related to subtle structural changes, despite the overall sequence similarity. These observations suggest a poor correlation between primary structure and biological activity or mode of action, when analyzing a large group of proteins with broad functional diversity such as the GH5 family.

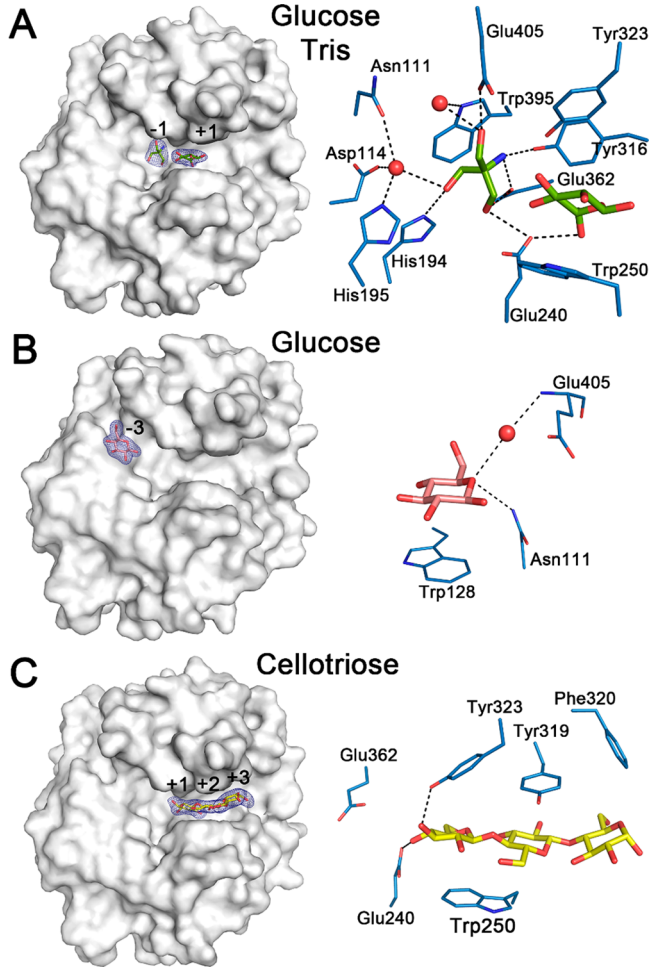

Figure 2. $XEG5A_{CD}$ complexes with glucose and Tris (A), glucose (B), and cellotriose (C). The $2F_o - F_c$ electron density maps contoured at 1σ of the ligands on the surface of XEG5A (left) and protein−ligand interactions (right) are shown.

DOI: 10.1021/acs.biochem.5b00011
Biochemistry 2015, 54, 1930−1942

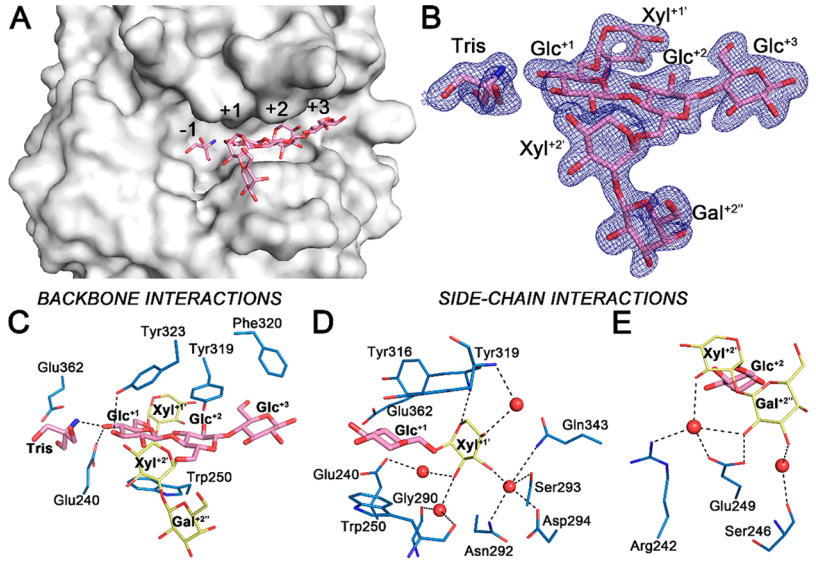

Figure 3. XEG5A$_{CD}$ in complex with XLG and Tris. (A) The xyloglucan oligosaccharide occupies the positive subsites (+1 to +3). (B) Depiction of the $2F_o - F_c$ electron density maps contoured at 1 σ of XLG and Tris. Schematic representation of the interactions made by XEG5A with backbone glucosyl residues (C), Xyl$^{+1'}$ (D) and, both Xyl$^{+2'}$ and Gal$^{+2''}$ (E).

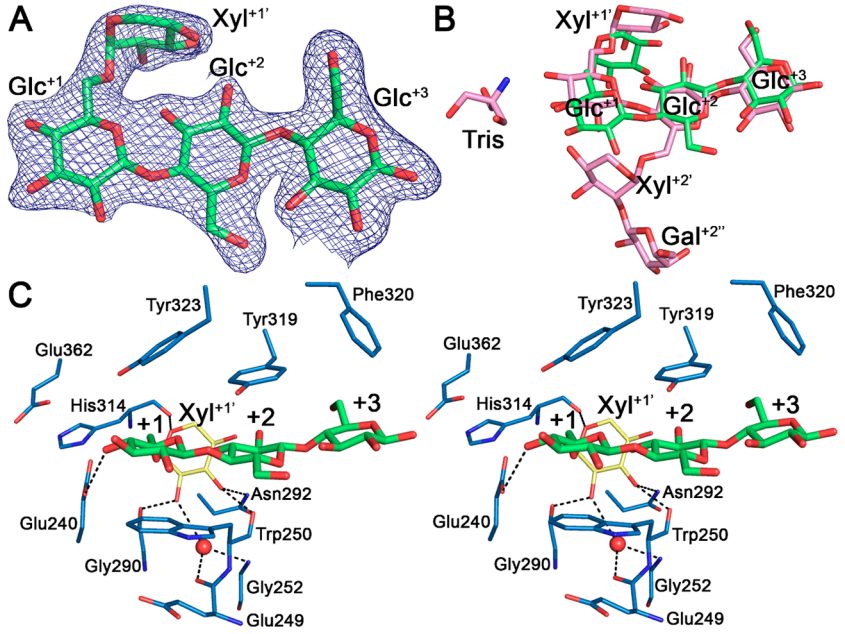

Figure 4. XEG5A$_{CD}$ in complex with XGG. (A) Representation of the $2F_o - F_c$ electron density map of the xyloglucan oligosaccharide contoured at 1σ. (B) Relative position of the oligosaccharides in the presence (pink) or absence of Tris (green). (C) Stereoview of protein-carbohydrate interactions.

Exploring the Sugar–Protein Interactions at the Positive Subsites of GH5 Xyloglucanases. Soaking of XEG5A$_{CD}$ crystals with glucose resulted in the occupation of the +1 subsite (Figure 2A). This monosaccharide makes stacking interactions with the side chain of Trp250 and a hydrogen bond with Glu240 (Figure 2A). In this complex, there is also a Tris molecule making several direct and water-mediated contacts with Asp114, His194, His195, Glu240, Tyr316, Glu362, Trp395, and Glu405; however, this ligand does not participate in the coordination of glucose (Figure 2A). In absence of Tris, the soaking with glucose resulted in the occupation of the −3 subsite (Figure 2B). Similarly to that observed in other GH5 XEGs,[30,31] this glucose is stabilized mainly by stacking interactions with Trp128 and additionally by hydrogen bonds with Asn111 (direct) and Glu405 (water-mediated) (Figure 2B).

There is a lack of structural data for the binding mode of xyloglucan to the positive subsites of GH5 XEGs. Therefore, the binding of cellotriose and xyloglucan oligosaccharides to these subsites in the XEG5A$_{CD}$ crystal (Figure S3) was instrumental to complete the mapping of the substrate-binding subsites of GH5 XEGs (Figures 2–4). Cellotriose was observed through the positives subsites from +1 to +3 (Figure 2C), with the binding mediated by sugar-aromatic interactions (Tyr319 and Trp250) and hydrogen bonds with Tyr323 and Glu240 (Figure 2C), as classically observed in GH5 cellulases complexes.

The xyloglucan-derived oligosaccharide used to soak XEG5A$_{CD}$ crystals was a mixture of XXXG, XXLG, XLXG,

DOI: 10.1021/acs.biochem.5b00011
Biochemistry 2015, 54, 1930–1942

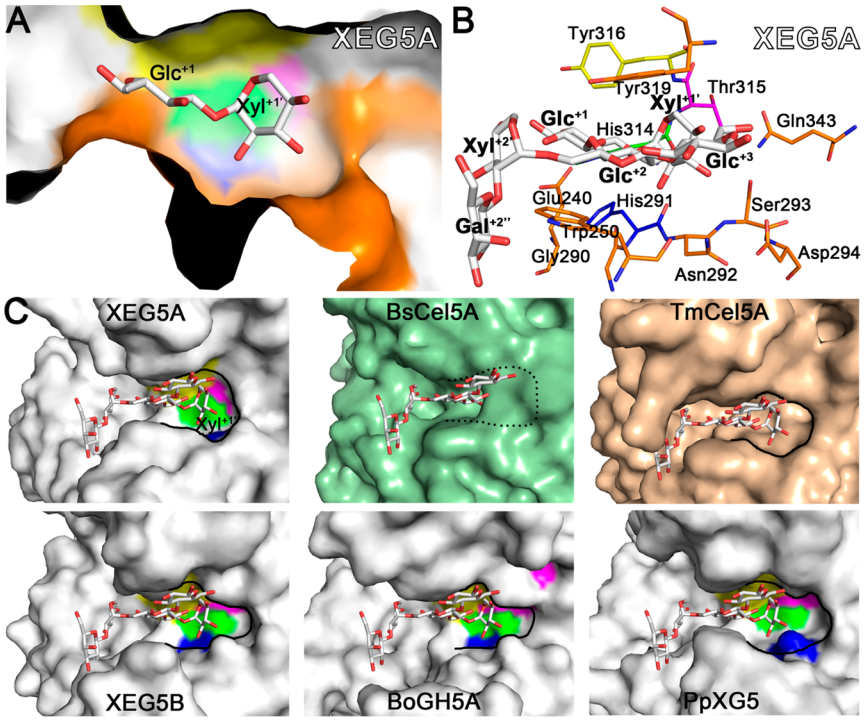

Figure 5. Pocket-like topology of the +1 subsite of GH5 XEGs. (A) Front view of the xylosyl residue at the +1 subsite of XEG5A. (B) Residues forming the +1 subsite of XEG5A. The structure of XEG5A has the same color pattern and similar orientations in panels A and B. (C) Side view of the region corresponding to the +1 subsite pocket (traced in black) of some GH5 enzymes discussed in this work. The only GH5 member in this panel without the pocket-like topology at the +1 subsite is BsCel5A (surface in green), which is not active on xyloglucan oligo- and polysaccharides.

and XLLG, which are end products of xyloglucan degradation by this enzyme.[28] In the presence of Tris, a strong electron density was observed spanning from +1 to +3 subsites (Figure 3A) where a XLG was modeled (Figure 3B). Thus, the ligand in the active site is either XLXG or XLLG. However, the lack of electron density did not permit modeling of $Xyl^{+3'}$ (and $Gal^{+3''}$, if it is the case) and Glc^{+4}, indicating these residues are nonproductive for substrate binding.

The side chains of Trp250, Tyr323, Tyr319, and Phe320 form an aromatic patch at the positive subsites for accommodation of the glucosyl main-chain residues (Glc^{+1}, Glc^{+2}, and Glc^{+3}) (Figure 3C). Interestingly, this set of residues is not conserved in other GH5 enzymes (Figure S2). Tyr323 is only observed in XEG5A and Phe320 is present in few enzymes (Figure S2). Trp250 is conserved in several GH5 enzymes, but this loop region differs between GH5 XEGs, PpXG5, and BoGH5A. The Glc^{+1} is additionally stabilized by hydrogen bonds with Tyr323OH, Glu240Oε2, and Tris (Figure 3C).

In contrast to the main-chain residues, the xylosyl substituents are mainly stabilized by polar interactions (Figure 3D,E). $Xyl^{+1'}$ interacts with the backbone nitrogen of Tyr316 and makes water-mediated hydrogen bonds with Glu240, Trp250, Gly290, Asn292, Ser293, Asp294, Tyr319, and Gln343 (Figure 3D). $Xyl^{+2'}$ only makes water-mediated interactions with Glu249 and Arg242, and its substituent, $Gal^{+2''}$, is hydrogen bonded to Glu249 and form water-mediated contacts with Ser246, Arg242, and Glu249 (Figure 3E).

In the absence of Tris, the oligosaccharide showed a slightly different conformation, in which the $Xyl^{+2'}$ substituent was not observed (Figure 4A–C). In this new complex, the Glc^{+1} does not interact with Tyr323OH (Figure 4C) and the O4 atom occupies the corresponding position of the Glc^{1+} O3 atom in the presence of Tris (Figure 4B). The displacement of Glc^{+1} consequently altered the position of $Xyl^{+1'}$ and new interactions are formed with Glu249 (water-mediated), Trp250, Gly252 (water-mediated), Gly290, Asn292, and His314 (Figure 4C). Glc^{+2} and Glc^{+3} are similar in both complexes.

Structural superposition of cellulases[54,55] and β-1,3-glucanases[56] on GH5 XEGs (including XEG5A (this work), XEG5B (this work), PpXG5[30] and BoGH5A[31]) indicates that the oligosaccharides occupy similar positions in the positive subsites of these proteins. All these enzymes present a narrow cleft at +1 and +2 subsites, delimited by aromatic side chains that interact with the carbohydrate by hydrophobic stacking. Then, the high-resolution mapping of the positive subsites of GH5 XEGs along with structural comparative analysis indicates a conserved mechanism for substrate backbone recognition among GH5 members, despite the distinct specificities.

Pocket-Like Topology of the +1 Subsite Is Conserved in GH5 Xyloglucan-Specific Endo-β-1,4-glucanases. The only two structures of GH5 xyloglucan-specific endo-β-1,4-glucanases available has limited our understanding of the structural determinants for xyloglucan specificity within this family, and the structural data of two novel GH5 XEGs, with low sequence similarity to those already reported, contributed to identify a conserved pocket-like topology of the +1 subsite for accommodation of the xylosyl moiety.

In XEG5A, $Xyl^{+1'}$ is accommodated by a pocket (Figure 5A) delimited by the residues Glu240, Trp250, Gly290, His291, Asn292, Ser293, Asp294, Hi314, Thr315, Tyr316, Tyr319, and Gln343 (Figure 5B). His291, His314, Thr315, and Tyr316 form the bottom of the pocket and the other residues delineate the borders of the pocket (Figure 5B). Glu240, His314, and Tyr316 are strictly conserved in the GH5 family, but the other residues are divergent (Figure S2), suggesting that this topology at the +1 subsite is particular to GH5 members with

DOI: 10.1021/acs.biochem.5b00011
Biochemistry 2015, 54, 1930–1942

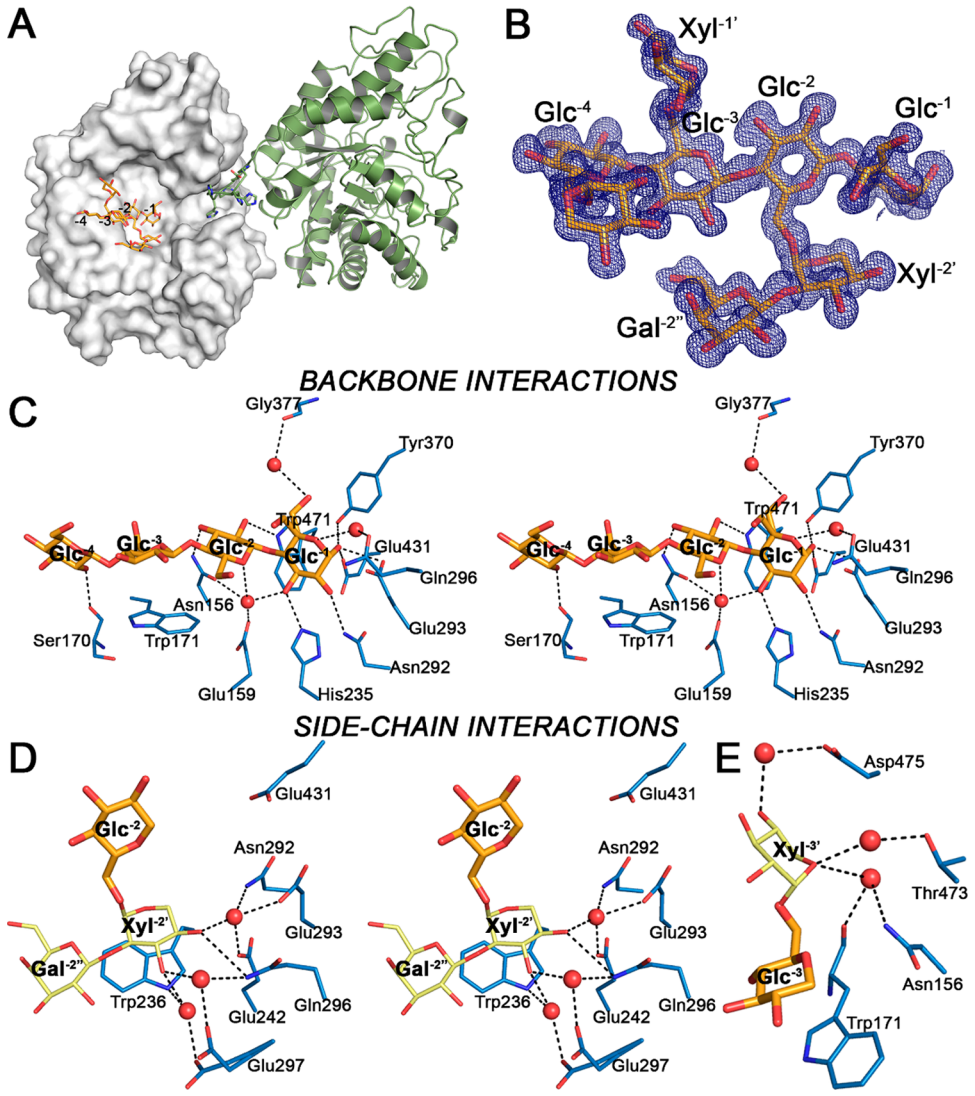

Figure 6. XEG5B$_{CD}$ structure in complex with XXLG. (A) The His-tag of a symmetry molecule (green) occludes the positive subsites of XEG5B, and the oligosaccharide XXLG (orange) occupies the negative subsites. (B) Representation of the $2F_o - F_c$ electron density map of XXLG contoured at 1σ. Interactions made by XEG5B with backbone glucosyl residues (C), Xyl$^{-2'}$ (D) and Xyl$^{-3'}$ (E).

preference for xyloglucan as substrate. Indeed, structural analysis of the structurally characterized XEGs, XEG5A (this work), XEG5B (this work), BoGH5A,[31] and PpXG5,[30] showed a deeper +1 subsite with the same pocket-like topology (Figure 5C). A similar pocket is present in the structure of the cellulase 5A from *Thermotoga maritima* (TmCel5A;[57] PDB ID: 3MMU; Figure 5C). This cellulase is capable of cleaving xyloglucan,[57] and, interestingly, the oligosaccharide from XEG5A complex could be well fitted into the TmCel5A pocket. On the other hand, GH5 members with very low or nondetectable activity on xyloglucan, for instance, the *Bacillus subtilis* cellulase 5A (BsCel5A,[58] PDB ID: 3PZT, Figure 5C), does not exhibit a pocket-like topology at the +1 subsite. Other GH5 enzymes have a deeper +1 subsite, such as PrEglA[53] (PDB ID: 3AYR), CtMult (PDB ID: 4IM4, unpublished data), the putative cellulase from *Prevotella bryantii* (PDB ID: 3VDH, unpublished data), and the endoglucanase A from *Clostridium cellulolyticum*[50] (PDB ID: 1EDG). However, these enzymes have not been characterized with respect to cleavage of branched substrates, precluding their systematic comparison with GH5 XEGs. On the basis of these analyses, we might suggest that the pocket-like topology of the +1 subsite strongly correlates with the ability to cleave xyloglucans, a common feature among the structurally characterized GH5 xyloglucan-specific endo-β-1,4-glucanases.

XEG5B Structure and Mapping of Negative Subsites. The full-length XEG5B was produced in *E. coli* cells in fusion with TRX at the N-terminus and with His-tag at the C-terminus. However, this construct did not yield crystals probably due to the flexibility conferred by the linker regions in the multimodular organization. Furthermore, this protein was found to be resistant to proteolysis, which prevented the use of the same strategy employed for XEG5A crystallization. Thus, for crystallographic purposes, the catalytic domain of XEG5B (XEG5B$_{CD}$) was cloned and overexpressed with a C-terminal His-tag. This construct showed high stability and promptly yielded crystals that diffracted up to 1.7 Å resolution (Table 1). The successful derivatization of XEG5B$_{CD}$ crystals with iodine anions permitted us to solve its structure by the SIRAS method (Table 1). As expected, the XEG5B$_{CD}$ structure exhibits a $(\beta/\alpha)_8$-barrel architecture (Figure 1A), and the eight invariant residues of GH5 enzymes[50,51] are conserved including Arg193, His235, Asn292, Glu293 (acid/base), His368, Tyr370,

DOI: 10.1021/acs.biochem.5b00011
Biochemistry 2015, 54, 1930−1942

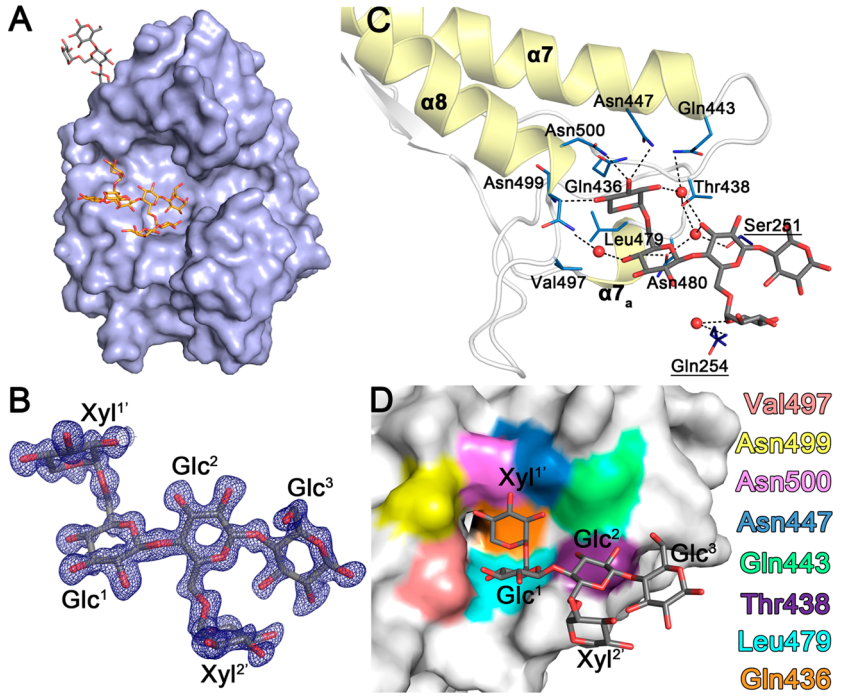

Figure 7. Surface binding site for xyloglucan oligosaccharide in XEG5B. (A) Location of the secondary binding site (XXG in gray) in relation to the catalytic interface (XXLG in orange). (B) Depiction of the $2F_o - F_c$ electron density map of XXG (contoured at 0.8σ). (C) Protein-carbohydrate interactions in the exosite. (D) Residues forming the surface binding site.

Glu431 (nucleophile) and Trp471 (XEG5B sequence numbering, Figures 1A and S2). In contrast to XEG5A, XEG5B showed highest similarity to the two structurally characterized GH5 XEGs, PpXG5[30] (PDB ID: 2JEP; r.m.s.d. 1.8 Å, 342 Cα atoms, 37% ident.) and BoGH5A[31] (PDB ID: 3ZMR; r.m.s.d. 2.0 Å, 345 Cα atoms, 30% ident.), and not to homologous cellulases from the GH5_4 subfamily. Preliminary homology modeling studies[29] suggested that an insertion in the β3-α3 loop (Phe246 to Thr262) would block one end of the active site conferring the unique mode of action of XEG5B within the GH5 family. However, the crystal structure of $XEG5B_{CD}$ showed that this loop does not obstruct the catalytic interface, and thus other structural elements are likely involved in its mode of action.

The crystal structure of $XEG5B_{CD}$ has been solved in the native form and in complex with xyloglucan oligosaccharide (Table 1). The r.m.s.d. of Cα atoms is 0.073 Å for superposed structures, and the main changes are in the side-chain conformations of residues interacting with the saccharides. Even though the positive subsites (+2 and +3 subsites) were obstructed by the His-tag of a symmetry molecule in the $XEG5B_{CD}$ crystal, the negative subsites were accessible, and one of the four xyloglucan-derived oligosaccharides (XXXG, XXLG, XLXG, and XLLG) bound to this region of the active site (Figure 6A). A galactosyl substituent cannot be accommodated by the −3 subsite due to steric impediments, whereas $Gal^{-2''}$ was modeled. Therefore, XLLG and XLXG are excluded, and XXLG is the only possible oligosaccharide attached to the negative subsites of this crystal packing. The good quality of the electron density map at 1.15 Å resolution permitted us to model all carbohydrate moieties of this ligand (Figure 6B). Glc^{-1} is hydrogen bonded to His235, Asn292, Glu431, Glu293, and Tyr370 (Figure 6C), and all these residues are strictly conserved in the GH5 family (Figure 1A and S2). This residue also makes water-mediated contacts with Glu159, Asn156, Gln296, and Gly377. At the −2 subsite, the glucosyl residue is interacting with Trp471, Asn156, and Glu159 (Figure 6C). Glc^{-3} makes stacking interactions with Trp471, whereas Glc^{-4} is only hydrogen bonded to the carbonyl oxygen of Ser170 (Figure 6C). The absence of hydrogen bonds with Glc^{-3} has also been reported for the two other GH5 XEGs, PpXG5,[30] and BoGH5A.[31] $Xyl^{-2'}$ is stacked with Trp236 and makes several water-mediated interactions with Asn292, Glu293, Glu242, Trp236, Glu297, and Gln296 (Figure 6D). In the native structure, a glycerol molecule occupies the position corresponding to $Xyl^{-2'}$. $Xyl^{-3'}$ only interacts with the protein (Thr473, Asn156, Trp171, and Asp475) through solvent molecules (Figure 6E). $Xyl^{-4'}$ and $Gal^{-2''}$ exclusively make intramolecular hydrogen bonds with other XXLG residues.

In comparison with the PpXG5 complex, the xyloglucan oligosaccharide has a similar binding mode, preserving the relative positions of $Xyl^{-2'}$, $Gal^{-2''}$, and $Xyl^{-3'}$ (Figure S4). However, only in the XEG5B complex the residues $Xyl^{-4'}$ is visible. In the BoGH5A complex, the $Xyl^{-4'}$ moiety adopts a totally different conformation so that preventing the presence of $Gal^{-2''}$ in the position observed in the XEG5B complex (Figure S4). It is also worth noting that Glc^{-1} adopts an α-configuration in the XEG5B complex and a β-configuration in the PpXG5 complex[30] (PDB ID: 2JEQ). In the α-configuration, Glc^{-1} interacts with the nucleophile (Glu431 in XEG5B, 2.4 Å) and with the acid/base (Glu293 in XEG5B, 3.2 Å), while in the β-configuration this residue only interacts with the acid/base (Glu182 in 2JEQ, 2.2 Å).

A Secondary Carbohydrate Binding Site in XEG5B. A second xyloglucan oligosaccharide, bound to a remote site, was also observed in the XEG5B complex (Figure 7A). This surface (secondary) binding site (SBS) is located in a pocket delimited by the structural elements α7, $\alpha7_a$, and α8, which is approximately 20 Å far from the negative subsites (Figure 7A–D). The electron density map allowed us to build the oligosaccharide XXG (Figure 7B). Glc^{1} interacts via solvent molecules with Val497

DOI: 10.1021/acs.biochem.5b00011
Biochemistry 2015, 54, 1930–1942

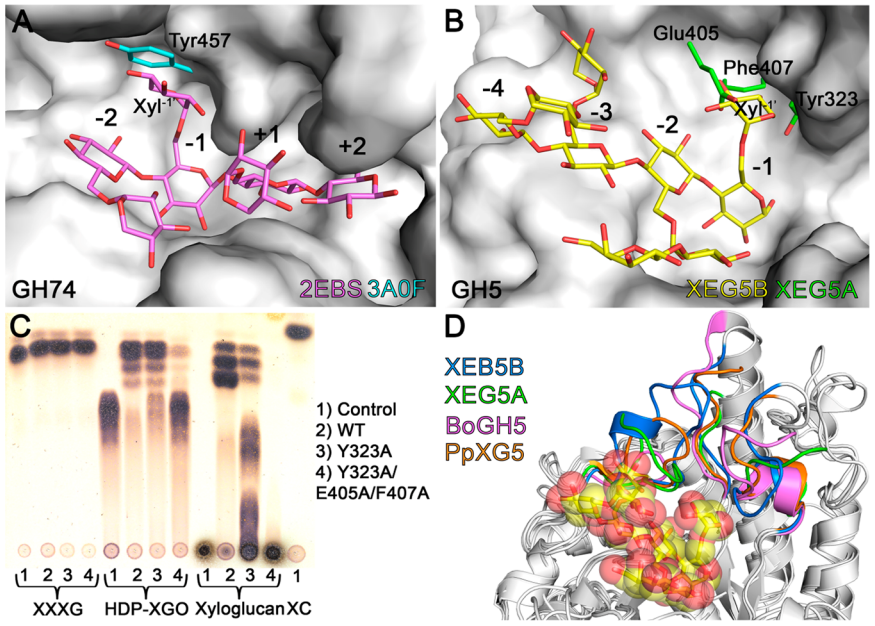

Figure 8. Accommodation of a xylosyl side chain in the −1 subsite determines the action mode of XEG5B. (A) The −1 subsite of the GH74 XEG from *Geotrichum* sp. M128 (PDB ID: 3A0F) has a tyrosine in the corresponding position of the $Xyl^{-1'}$ side chain in OXG-RCBH (PDB ID: 2EBS). (B) Similar to GH74 enzymes, the side chains of three residues of XEG5A occupy the corresponding $Xyl^{-1'}$-binding subsite present in XEG5B. (C) Thin-layer chromatographic analysis of hydrolytic activity of XEG5A mutants against XXXG, HDP-XGO, and xyloglucan. Xylosyl-cellobiose (XC, borohydride reduced, Megazyme, Wicklow, Ireland) is used as a molecular weight marker. (D) The −1 subsite of XEG5B is unique between structurally characterized GH5 XEGs.

(main-chain nitrogen atom), Thr438, and Asn480 (Figure 7C). Glc^2 is hydrogen bonded to Gln443, Thr438, and Asn480, whereas Glc^3 does make any contact with the protein (Figure 7C). $Xyl^{1'}$ is attached to Asn499, Asn500, and Asn447, and makes water-mediated interactions with Gln443 and Thr438 (Figure 7C). $Xyl^{2'}$ only interacts with Gln254. Among all residues forming this SBS, only Asn447 and Asn500 are conserved in PpXG5, and this pocket is not present in other structurally characterized GH5 XEGs, indicating it to be a particular feature of XEG5B.

SBSs have been identified in approximately 50 carbohydrate-active enzymes (http://www.cazypedia.org/index.php/Surface_Binding_Site), and according to the literature,[59] they might function as allosteric regulators, pseudo-CBMs, or extensions of the active site. Besides XEG5B, only in the crystal structure of the exo-β-1,3-glucanase from *Candida albicans*[56] was observed an SBS within the GH5 family. The SBS in this enzyme is located at the opposite face of the active site and differs from the XEG5B SBS. In the *C. albicans* exo-β-1,3-glucanase, the presence of this exosite was suggested to assist the association of the enzyme with branched glucans of the *C. albicans* cell wall,[56] and in XEG5B, it may have a role in targeting the enzyme to the cellulose-xyloglucan complex.

Structural Basis for α-D-Xyl*p*(1 → 6)-D-Glc*p* Recognition at the −1 Subsite by XEG5B. XEG5B only cleaves xyloglucan and does not act on unbranched glucans, suggesting that side-chain substitutions are needed for substrate recognition.[29] The end products of HDP-XGO hydrolysis by XEG5B are XX and XG, and the enzyme cleaves XXXG into XX and XG, indicating that cleavage occurred at branched D-glucopyranosyl residues.[29] This property of cleaving at branched residues has been reported for a few GH74 enzymes: oligoxyloglucan reducing-end-specific cellobiohydrolase (OXG-RCBH) from *Geotrichum* sp. M128,[26] Cel74A from *Hypocrea jecorina*,[22] and an endoxyloglucanase from *Xanthomonas citri* pv *Mangiferaeindicae*.[33] The three-dimensional structure of Cel74A has not been solved to date, but enzymatic assays indicate that its active center is composed of at least four subsites and that the enzyme is not able to hydrolyze xyloglucan at unbranched glucosyl residues.[22] The *Xanthomonas* XEG structure is also unknown, but the cleavage pattern showed that the enzyme has an absolute requirement for a xylosyl side chain at the −1 subsite.[33] The structure in complex with XXXG (spanning from −2 to +2 subsites) clearly shows that OXG-RCBH recognizes a xylosyl moiety at the −1 subsite via the residue Asn488.[60] A XEG from *Geotrichum* sp. M128, that is very similar to OXG-RCBH (48% identity), has the −1 subsite occupied by Tyr457[61] (Figure 8A), and the Y457G variant cleaved the xyloglucan oligosaccharide at various sites (X↓X↓X↓G↓X↓X↓XG) instead of the only site (XXXG↓XXXG) cleaved by the wild-type enzyme, which confirmed the importance of the −1 subsite topology for its mode of action.[61]

XEG5B has a wide cleft around the −1 subsite (Figure 8B), similar to that observed for OXG-RCBH[60] (Figure 8A). Although there is no XEG5B−xyloglucan complex with $Xyl^{-1'}$, molecular modeling indicates that this carbohydrate moiety might be accommodated by the −1 subsite of XEG5B (Figure 8B). Moreover, superposition of XEG5A on XEG5B structure showed that at least three residues of XEG5A occupy the corresponding volume of $Xyl^{-1'}$: Tyr323, Glu405, and Phe407 (Figure 8B). In an attempt to confirm that the aperture of this cleft contributes to substrate specificity and cleavage pattern, these three residues of XEG5A were mutated to alanine. The Y323A mutant presented similar catalytic activity to that observed for the wild-type enzyme, being active on tamarind seed xyloglucan polysaccharide and HDP-XGO, but not cleaving XXXG (Figure 8C). The triple mutant (Y323A/E405A/F407A) did not cleave any of the tested substrates (Figure 8C), demonstrating that these

DOI: 10.1021/acs.biochem.5b00011
Biochemistry 2015, 54, 1930−1942

substitutions abolished the enzymatic activity of XEG5A probably due to extensive perturbation of the active site. Structural analysis revealed that the $Xyl^{-1'}$-binding subsite in XEG5B, formed by the loops β6-α6, β7-α7, and β8-α8, is unique in both amino-acid composition (Figure S2) and three-dimensional structure (Figure 8D), corroborating that those side-chain mutations would not be sufficient to mimic the −1 subsite of XEG5B in XEG5A. Nevertheless, the structural evidence presented here are as much as necessary to support an important role of these adaptations in the −1 subsite of XEG5B for XXXG cleavage into XX and XG.

Xyloglucan hydrolysis by XEGs usually produces hepta (XXXG), octa (XLXG or XXLG), and nonasaccharides (XLLG)[28,30,31,62−64] indicating that cleavage occurs between an unbranched and a branched glucopyranosyl residue. The end products of HDP-XGO hydrolysis by XEG5B are XX and XG, which suggests the following cleavage pattern···XX↓XG↓XX↓XG···. On the basis of this mode of action, we can assume that the enzyme can accept both branched and unbranched glucopyranosyl residues at −1 and +2 subsites, whereas at −2 and +1 subsites there is always a branched residue.

These observations indicate that side-chain residues at −2 and +1 subsites are important for substrate binding and corroborate with biochemical and structural data available for other GH5 XEGs.[30,31] As discussed above, the binding of a xylosyl side chain at the +1 subsite pocket seems to be essential for substrate binding and catalysis in XEGs. Moreover, stacking interactions with $Xyl^{-2'}$ are present in XEG5B, PpXG5, and BoGH5A, enzymes only active on branched polysaccharides,[29−31] suggesting a relevant role of this interaction for substrate recognition. On the other hand, the side-chain substitutions at the +2 subsite are not strictly necessary for substrate binding as supported by XEG5A−xyloglucan complex, in which the Glc^{+2} is strongly stabilized by stacking interactions with Trp250 and Tyr319, and its xylosyl substituent points outside the catalytic cleft (Figure 3A). At the −1 subsite, only XEG5B can accommodate a xylosyl side-chain among the GH5 XEGs. But similarly to that observed for the +2 subsite, the presence of $Xyl^{-1'}$ is not essential for substrate interaction. In this case, the numerous interactions made by backbone glucosyl residues (Figure 6C) would be sufficient for correct assignment.

In addition, the cleavage of XXXG by XEG5B[29] indicates that this oligosaccharide has the minimal requirements for productive interactions leading to hydrolysis. This is in agreement with the few interactions made by XEG5B with the xyloglucan oligosaccharide at −3 and −4 subsites (Figure 6C). Moreover, according to XEG5A complex structure, the +3 subsite of XEG5B should not make interactions with the substrate. Thus, our structural analyses show that the active site of XEG5B is constituted by four high-affinity subsites (−2 to +2), and, for correct substrate binding in this cleft, side-chain substitutions at −2 and +1 subsites are strictly necessary. In this way, linear polymers, such as β-glucan, CMC, and lichenin constitute "poor" substrates for XEG5B, which is in accordance with nondetectable activity on these polysaccharides.[29]

CONCLUDING REMARKS

Xyloglucan differs from cellulose by the presence of a regular pattern of substitutions at the C6 position of the backbone glucopyranosyl residues. The classification of a glycoside hydrolase as a cellulase or XEG depends on the best substrate for that enzyme.[32] Despite their preference, enzymes may also cleave other substrates with lower catalytic efficiency. Cellulases have a preference for linear polysaccharides, but some of them may also hydrolyze xyloglucan. In this case, they merely tolerate branched substrates. XEGs are the enzymes with a catalytic preference for xyloglucan. Their active site accommodates xyloglucan saccharides, making interactions with both carbohydrate backbone and side-chain moieties. Some XEGs also cleave linear polysaccharides, possibly due to the presence of sufficient interactions with the backbone to permit hydrolysis, but in a much less productive way.

In this study, we solved the structures of two novel GH5 XEGs in complex with xyloglucan oligosaccharides and other ligands. The oligosaccharide found in the XEG5A complex permitted us to map, for the first time, the positive subsites of a GH5 XEG. This complex also showed that the pocket-like topology of the +1 subsite is essential for the binding of a xylosyl side chain, which probably has an important role in substrate recognition by GH5 XEGs. The oligosaccharide found in the XEG5B complex along with extensive structural analyses revealed the structural basis for XXXG hydrolysis, which involves a modification in the −1 subsite, enabling the accommodation of a xylosyl moiety at this position.

In summary, this work provides a complete high-resolution subsite mapping of GH5 XEGs and sheds light on the structural determinants for their mode of action and how they recognize and bind to branched substrates. These enzymes have great importance in the conversion of lignocellulose into fermentable sugars, especially when dicotyledons are the source of the biomass.

ASSOCIATED CONTENT

Supporting Information

The magnesium ion coordination in the XEG5A structure (Figure S1), multiple sequence alignment of GH5 enzymes (Figure S2), the occlusion of the negative subsites by a symmetry molecule in the XEG5A crystal structure (Figure S3), and the binding mode of xyloglucan oligosaccharides in the negative subsites of XEG5B, BoGH5A and PpXG5 (Figure S4). This material is available free of charge via the Internet at http://pubs.acs.org.

AUTHOR INFORMATION

Corresponding Author

*Address: Brazilian Biosciences National Laboratory, Brazilian Center of Research in Energy and Materials, Giuseppe Maximo Scolfaro 10000, 13083-970, Campinas, SP, Brazil. Tel 55-19-3512-1106. Fax 55-19-3512-1100. E-mail: mario.murakami@lnbio.cnpem.br.

Author Contributions

#Both authors (C.R.d.S. and R.L.C.) have contributed equally to this work.

Funding

This research was supported by Fundação de Amparo à Pesquisa do Estado de São Paulo (FAPESP) [Grant Nos. 10/51890-8 and 13/13309-0 to M.T.M.], Conselho Nacional de Desenvolvimento Científico e Tecnológico (CNPq) [Grant Numbers 476043/2011-5 and 308092/2012-0 to M.T.M.], and Coordenação de Aperfeiçoamento de Pessoal de Nível Superior (CAPES).

Notes

The authors declare no competing financial interest.

DOI: 10.1021/acs.biochem.5b00011
Biochemistry 2015, 54, 1930−1942

■ ACKNOWLEDGMENTS

We are thankful to National Center for Research in Energy and Materials (CNPEM - LNLS and LNBio) for the provision of time at the MX2 Beamline, crystallization (Robolab) and spectroscopy (LEC) facilities.

■ ABBREVIATIONS

PpXG5, XG5 from *Paenibacillus pabuli*; BoGH5A, GH5A from *Bacteroides ovatus*; BsCel5A, cellulase 5A from *Bacillus subtilis*; CAZy, carbohydrate-Active enZYmes; CMC, carboxymethyl cellulose; CtMult, multifunctional cellulase, xylanase, and mannanase from *Clostridium thermocellum*; HDP-XGO, high degree of polymerization xyloglucan oligosaccharide; OXG-RCBH, oligoxyloglucan reducing-end-specific cellobiohydrolase from *Geotrichum* sp. M128; PrEglA, endoglucanase EglA from *Piromyces rhizinflat*; SAD, single anomalous dispersion; SBS, surface binding subsite; SIRAS, single isomorphous replacement with anomalous scattering; TRX, thioredoxin; XEG, xyloglucan-specific endo-β-1,4-glucanase; $XEG5A_{CD}$, catalytic domain of XEG5A; $XEG5B_{CD}$, catalytic domain of XEG5B

■ REFERENCES

(1) Fry, S. C. (1989) The Structure and Functions of Xyloglucan. *J. Exp. Bot. 40*, 1−11.
(2) Popper, Z. A., and Fry, S. C. (2003) Primary cell wall composition of bryophytes and charophytes. *Ann. Bot. 91*, 1−12.
(3) Popper, Z. A., and Fry, S. C. (2004) Primary cell wall composition of pteridophytes and spermatophytes. *New Phytol. 164*, 165−174.
(4) Sarkar, P., Bosneaga, E., and Auer, M. (2009) Plant cell walls throughout evolution: towards a molecular understanding of their design principles. *J. Exp. Bot. 60*, 3615−3635.
(5) Tuomivaara, S. T., Yaoi, K., O'Neill, M. A., and York, W. S. (2015) Generation and structural validation of a library of diverse xyloglucan-derived oligosaccharides, including an update on xyloglucan nomenclature. *Carbohydr. Res. 402*, 56−66.
(6) Vincken, J. P., York, W. S., Beldman, G., and Voragen, A. G. (1997) Two general branching patterns of xyloglucan, XXXG and XXGG. *Plant Physiol. 114*, 9−13.
(7) Carpita, N. C., and Gibeaut, D. M. (1993) Structural models of primary cell walls in flowering plants: consistency of molecular structure with the physical properties of the walls during growth. *Plant J. 3*, 1−30.
(8) Pauly, M., Albersheim, P., Darvill, A., and York, W. S. (1999) Molecular domains of the cellulose/xyloglucan network in the cell walls of higher plants. *Plant J. 20*, 629−639.
(9) Cosgrove, D. J. (2005) Growth of the plant cell wall. *Nat. Rev. Mol. Cell Biol. 6*, 850−861.
(10) Buckeridge, M. S., Pessoa dos Santos, H., and Tiné, M. A. S. (2000) Mobilisation of storage cell wall polysaccharides in seeds. *Plant Physiol. Biochem. 38*, 141−156.
(11) Scheible, W. R., and Pauly, M. (2004) Glycosyltransferases and cell wall biosynthesis: novel players and insights. *Curr. Opin. Plant Biol. 7*, 285−295.
(12) Miyazaki, S., Suisha, F., Kawasaki, N., Shirakawa, M., Yamatoya, K., and Attwood, D. (1998) Thermally reversible xyloglucan gels as vehicles for rectal drug delivery. *J. Controlled Release 56*, 75−83.
(13) Brumer, H., 3rd, Zhou, Q., Baumann, M. J., Carlsson, K., and Teeri, T. T. (2004) Activation of crystalline cellulose surfaces through the chemoenzymatic modification of xyloglucan. *J. Am. Chem. Soc. 126*, 5715−5721.
(14) Zhou, Q., Baumann, M. J., Brumer, H., and Teeri, T. T. (2006) The influence of surface chemical composition on the adsorption of xyloglucan to chemical and mechanical pulps. *Carbohydr. Polym. 63*, 449−458.
(15) Zhou, Q., Greffe, L., Baumann, M. J., Malmström, E., Teeri, T. T., and Brumer, H. (2005) Use of Xyloglucan as a Molecular Anchor for the Elaboration of Polymers from Cellulose Surfaces: A General Route for the Design of Biocomposites. *Macromolecules 38*, 3547−3549.
(16) Greffe, L., Bessueille, L., Bulone, V., and Brumer, H. (2005) Synthesis, preliminary characterization, and application of novel surfactants from highly branched xyloglucan oligosaccharides. *Glycobiology 15*, 437−445.
(17) Hoffman, M., Jia, Z., Pena, M. J., Cash, M., Harper, A., Blackburn, A. R., 2nd, Darvill, A., and York, W. S. (2005) Structural analysis of xyloglucans in the primary cell walls of plants in the subclass Asteridae. *Carbohydr. Res. 340*, 1826−1840.
(18) Menon, V., Prakash, G., and Rao, M. (2010) Enzymatic hydrolysis and ethanol production using xyloglucanase and Debaromyces hansenii from tamarind kernel powder: galactoxyloglucan predominant hemicellulose. *J. Biotechnol. 148*, 233−239.
(19) Lombard, V., Golaconda Ramulu, H., Drula, E., Coutinho, P. M., and Henrissat, B. (2014) The carbohydrate-active enzymes database (CAZy) in 2013. *Nucleic Acids Res. 42*, D490−495.
(20) Davies, G. J., Wilson, K. S., and Henrissat, B. (1997) Nomenclature for sugar-binding subsites in glycosyl hydrolases. *Biochem. J. 321* (Pt 2), 557−559.
(21) Yaoi, K., Nakai, T., Kameda, Y., Hiyoshi, A., and Mitsuishi, Y. (2005) Cloning and characterization of two xyloglucanases from Paenibacillus sp. strain KM21. *Appl. Environ. Microbiol. 71*, 7670−7678.
(22) Desmet, T., Cantaert, T., Gualfetti, P., Nerinckx, W., Gross, L., Mitchinson, C., and Piens, K. (2007) An investigation of the substrate specificity of the xyloglucanase Cel74A from Hypocrea jecorina. *FEBS J. 274*, 356−363.
(23) Ichinose, H., Araki, Y., Michikawa, M., Harazono, K., Yaoi, K., Karita, S., and Kaneko, S. (2012) Characterization of an endo-processive-type xyloglucanase having a beta-1,4-glucan-binding module and an endo-type xyloglucanase from Streptomyces avermitilis. *Appl. Environ. Microbiol. 78*, 7939−7945.
(24) Feng, T., Yan, K. P., Mikkelsen, M. D., Meyer, A. S., Schols, H. A., Westereng, B., and Mikkelsen, J. D. (2014) Characterisation of a novel endo-xyloglucanase (XcXGHA) from Xanthomonas that accommodates a xylosyl-substituted glucose at subsite −1. *Appl. Microbiol. Biotechnol. 98*, 9667−9679.
(25) Ariza, A., Eklof, J. M., Spadiut, O., Offen, W. A., Roberts, S. M., Besenmatter, W., Friis, E. P., Skjot, M., Wilson, K. S., Brumer, H., and Davies, G. (2011) Structure and activity of *Paenibacillus polymyxa* xyloglucanase from glycoside hydrolase family 44. *J. Biol. Chem. 286*, 33890−33900.
(26) Yaoi, K., and Mitsuishi, Y. (2002) Purification, characterization, cloning, and expression of a novel xyloglucan-specific glycosidase, oligoxyloglucan reducing end-specific cellobiohydrolase. *J. Biol. Chem. 277*, 48276−48281.
(27) Bauer, S., Vasu, P., Mort, A. J., and Somerville, C. R. (2005) Cloning, expression, and characterization of an oligoxyloglucan reducing end-specific xyloglucanobiohydrolase from *Aspergillus nidulans*. *Carbohydr. Res. 340*, 2590−2597.
(28) Wong, D. D., Chan, V. J., McCormack, A. A., and Batt, S. B. (2010) A novel xyloglucan-specific endo-beta-1,4-glucanase: biochemical properties and inhibition studies. *Appl. Microbiol. Biotechnol. 86*, 1463−1471.
(29) Wong, D. D., Chan, V. J., McCormack, A. A., and Batt, S. B. (2010) Cloning and characterization of an exo-xylogucanase from rumenal microbial metagenome. *Protein Pept. Lett. 17*, 803−808.
(30) Gloster, T. M., Ibatullin, F. M., Macauley, K., Eklof, J. M., Roberts, S., Turkenburg, J. P., Bjornvad, M. E., Jorgensen, P. L., Danielsen, S., Johansen, K. S., Borchert, T. V., Wilson, K. S., Brumer, H., and Davies, G. J. (2007) Characterization and three-dimensional structures of two distinct bacterial xyloglucanases from families GH5 and GH12. *J. Biol. Chem. 282*, 19177−19189.
(31) Larsbrink, J., Rogers, T. E., Hemsworth, G. R., McKee, L. S., Tauzin, A. S., Spadiut, O., Klinter, S., Pudlo, N. A., Urs, K., Koropatkin,

DOI: 10.1021/acs.biochem.5b00011
Biochemistry 2015, 54, 1930−1942

N. M., Creagh, A. L., Haynes, C. A., Kelly, A. G., Cederholm, S. N., Davies, G. J., Martens, E. C., and Brumer, H. (2014) A discrete genetic locus confers xyloglucan metabolism in select human gut Bacteroidetes. *Nature 506*, 498−502.
(32) Eklof, J. M., Ruda, M. C., and Brumer, H. (2012) Distinguishing xyloglucanase activity in endo-beta(1−>4)glucanases. *Methods Enzymol. 510*, 97−120.
(33) Feng, T., Yan, K. P., Mikkelsen, M. D., Meyer, A. S., Schols, H. A., Westereng, B., and Mikkelsen, J. D. (2014) Characterisation of a novel endo-xyloglucanase (XcXGHA) from Xanthomonas that accommodates a xylosyl-substituted glucose at subsite −1. *Appl. Microbiol. Biotechnol. 98*, 9667−9679.
(34) Doublie, S. (2007) Production of selenomethionyl proteins in prokaryotic and eukaryotic expression systems. *Methods Mol. Biol. 363*, 91−108.
(35) Van Duyne, G. D., Standaert, R. F., Karplus, P. A., Schreiber, S. L., and Clardy, J. (1993) Atomic structures of the human immunophilin FKBP-12 complexes with FK506 and rapamycin. *J. Mol. Biol. 229*, 105−124.
(36) Doublie, S. (1997) Preparation of selenomethionyl proteins for phase determination. *Methods Enzymol. 276*, 523−530.
(37) McPhillips, T. M., McPhillips, S. E., Chiu, H. J., Cohen, A. E., Deacon, A. M., Ellis, P. J., Garman, E., Gonzalez, A., Sauter, N. K., Phizackerley, R. P., Soltis, S. M., and Kuhn, P. (2002) Blu-Ice and the Distributed Control System: software for data acquisition and instrument control at macromolecular crystallography beamlines. *J. Synchrotron Radiat. 9*, 401−406.
(38) Evans, G., and Pettifer, R. F. (2001) CHOOCH: a program for deriving anomalous-scattering factors from X-ray fluorescence spectra. *J. Appl. Crystallogr. 34*, 82−86.
(39) Dauter, Z., Dauter, M., and Rajashankar, K. R. (2000) Novel approach to phasing proteins: derivatization by short cryo-soaking with halides. *Acta Crystallogr., Sect. D Biol. Crystallogr. 56*, 232−237.
(40) Guimaraes, B. G., Sanfelici, L., Neuenschwander, R. T., Rodrigues, F., Grizolli, W. C., Raulik, M. A., Piton, J. R., Meyer, B. C., Nascimento, A. S., and Polikarpov, I. (2009) The MX2 macromolecular crystallography beamline: a wiggler X-ray source at the LNLS. *J. Synchrotron Radiat. 16*, 69−75.
(41) Kabsch, W. (2010) Xds. *Acta Crystallogr., Sect. D, Biol. Crystallogr. 66*, 125−132.
(42) Karplus, P. A., and Diederichs, K. (2012) Linking crystallographic model and data quality. *Science 336*, 1030−1033.
(43) Sheldrick, G. M. (2010) Experimental phasing with SHELXC/D/E: combining chain tracing with density modification. *Acta Crystallogr., Sect. D Biol. Crystallogr. 66*, 479−485.
(44) Terwilliger, T. C., Grosse-Kunstleve, R. W., Afonine, P. V., Moriarty, N. W., Zwart, P. H., Hung, L. W., Read, R. J., and Adams, P. D. (2008) Iterative model building, structure refinement and density modification with the PHENIX AutoBuild wizard. *Acta Crystallogr., Sect. D Biol. Crystallogr. 64*, 61−69.
(45) Vagin, A., and Teplyakov, A. (2010) Molecular replacement with MOLREP. *Acta Crystallogr.. Sect. D Biol. Crystallogr. 66*, 22−25.
(46) Murshudov, G. N., Vagin, A. A., and Dodson, E. J. (1997) Refinement of macromolecular structures by the maximum-likelihood method. *Acta Crystallogr., Sect. D Biol. Crystallogr. 53*, 240−255.
(47) Emsley, P., Lohkamp, B., Scott, W. G., and Cowtan, K. (2010) Features and development of Coot. *Acta Crystallogr., Sect. D Biol. Crystallogr. 66*, 486−501.
(48) Chen, V. B., Arendall, W. B., 3rd, Headd, J. J., Keedy, D. A., Immormino, R. M., Kapral, G. J., Murray, L. W., Richardson, J. S., and Richardson, D. C. (2010) MolProbity: all-atom structure validation for macromolecular crystallography. *Acta Crystallogr., Sect. D Biol. Crystallogr. 66*, 12−21.
(49) Terwilliger, T. C., Dimaio, F., Read, R. J., Baker, D., Bunkoczi, G., Adams, P. D., Grosse-Kunstleve, R. W., Afonine, P. V., and Echols, N. (2012) phenix.mr_rosetta: molecular replacement and model rebuilding with Phenix and Rosetta. *J. Struct. Funct. Genomics 13*, 81−90.
(50) Ducros, V., Czjzek, M., Belaich, A., Gaudin, C., Fierobe, H. P., Belaich, J. P., Davies, G. J., and Haser, R. (1995) Crystal structure of the catalytic domain of a bacterial cellulase belonging to family 5. *Structure 3*, 939−949.
(51) Bianchetti, C. M., Brumm, P., Smith, R. W., Dyer, K., Hura, G. L., Rutkoski, T. J., and Phillips, G. N., Jr. (2013) Structure, dynamics, and specificity of endoglucanase D from *Clostridium cellulovorans*. *J. Mol. Biol. 425*, 4267−4285.
(52) Aspeborg, H., Coutinho, P. M., Wang, Y., Brumer, H., 3rd, and Henrissat, B. (2012) Evolution, substrate specificity and subfamily classification of glycoside hydrolase family 5 (GH5). *BMC Evol. Biol. 12*, 186.
(53) Tseng, C. W., Ko, T. P., Guo, R. T., Huang, J. W., Wang, H. C., Huang, C. H., Cheng, Y. S., Wang, A. H., and Liu, J. R. (2011) Substrate binding of a GH5 endoglucanase from the ruminal fungus *Piromyces rhizinflata*. *Acta Crystallogr., Sect. F Struct. Biol. Cryst. Commun. 67*, 1189−1194.
(54) Kim, H. W., and Ishikawa, K. (2011) Functional analysis of hyperthermophilic endocellulase from *Pyrococcus horikoshii* by crystallographic snapshots. *Biochem. J. 437*, 223−230.
(55) Sakon, J., Adney, W. S., Himmel, M. E., Thomas, S. R., and Karplus, P. A. (1996) Crystal structure of thermostable family 5 endocellulase E1 from *Acidothermus cellulolyticus* in complex with cellotetraose. *Biochemistry 35*, 10648−10660.
(56) Patrick, W. M., Nakatani, Y., Cutfield, S. M., Sharpe, M. L., Ramsay, R. J., and Cutfield, J. F. (2010) Carbohydrate binding sites in Candida albicans exo-beta-1,3-glucanase and the role of the Phe-Phe 'clamp' at the active site entrance. *FEBS J. 277*, 4549−4561.
(57) Pereira, J. H., Chen, Z., McAndrew, R. P., Sapra, R., Chhabra, S. R., Sale, K. L., Simmons, B. A., and Adams, P. D. (2010) Biochemical characterization and crystal structure of endoglucanase Cel5A from the hyperthermophilic *Thermotoga maritima*. *J. Struct. Biol. 172*, 372−379.
(58) Santos, C. R., Paiva, J. H., Sforca, M. L., Neves, J. L., Navarro, R. Z., Cota, J., Akao, P. K., Hoffmam, Z. B., Meza, A. N., Smetana, J. H., Nogueira, M. L., Polikarpov, I., Xavier-Neto, J., Squina, F. M., Ward, R. J., Ruller, R., Zeri, A. C., and Murakami, M. T. (2012) Dissecting structure-function-stability relationships of a thermostable GH5-CBM3 cellulase from *Bacillus subtilis* 168. *Biochem. J. 441*, 95−104.
(59) Cuyvers, S., Dornez, E., Delcour, J. A., and Courtin, C. M. (2012) Occurrence and functional significance of secondary carbohydrate binding sites in glycoside hydrolases. *Crit. Rev. Biotechnol. 32*, 93−107.
(60) Yaoi, K., Kondo, H., Hiyoshi, A., Noro, N., Sugimoto, H., Tsuda, S., Mitsuishi, Y., and Miyazaki, K. (2007) The structural basis for the exo-mode of action in GH74 oligoxyloglucan reducing end-specific cellobiohydrolase. *J. Mol. Biol. 370*, 53−62.
(61) Yaoi, K., Kondo, H., Hiyoshi, A., Noro, N., Sugimoto, H., Tsuda, S., and Miyazaki, K. (2009) The crystal structure of a xyloglucan-specific endo-beta-1,4-glucanase from Geotrichum sp. M128 xyloglucanase reveals a key amino acid residue for substrate specificity. *FEBS J. 276*, 5094−5100.
(62) Damasio, A. R., Ribeiro, L. F., Ribeiro, L. F., Furtado, G. P., Segato, F., Almeida, F. B., Crivellari, A. C., Buckeridge, M. S., Souza, T. A., Murakami, M. T., Ward, R. J., Prade, R. A., and Polizeli, M. L. (2012) Functional characterization and oligomerization of a recombinant xyloglucan-specific endo-beta-1,4-glucanase (GH12) from *Aspergillus niveus*. *Biochim. Biophys. Acta 1824*, 461−467.
(63) Martinez-Fleites, C., Guerreiro, C. I., Baumann, M. J., Taylor, E. J., Prates, J. A., Ferreira, L. M., Fontes, C. M., Brumer, H., and Davies, G. J. (2006) Crystal structures of *Clostridium thermocellum* xyloglucanase, XGH74A, reveal the structural basis for xyloglucan recognition and degradation. *J. Biol. Chem. 281*, 24922−24933.
(64) Master, E. R., Zheng, Y., Storms, R., Tsang, A., and Powlowski, J. (2008) A xyloglucan-specific family 12 glycosyl hydrolase from *Aspergillus niger*: recombinant expression, purification and characterization. *Biochem. J. 411*, 161−170.

DOI: 10.1021/acs.biochem.5b00011
Biochemistry 2015, 54, 1930−1942